Bulletin of the Seismological Society of America, Vol. 80, No. 5, pp. 1374–1381, October 1990

*SHORT NOTES*

# SEISMICITY AS A FUNCTION OF CUMULATIVE GEOLOGIC OFFSET: SOME OBSERVATIONS FROM SOUTHERN CALIFORNIA

BY STEVEN G. WESNOUSKY

It has been recognized for some time now that the character of seismicity varies significantly between the major strike-slip fault zones of California (e.g., Allen, 1968). The San Andreas fault, for example, site of two of the largest earthquakes in California history (in 1857 and 1906), has been virtually aseismic at the microearthquake level along much of the fault length during the last 50 to 60 years (Figs. 1, 2, and 3). In contrast, the San Jacinto fault has produced numerous moderate earthquakes of magnitude 6 to 7 and shows an abundance of microearthquake activity. The cumulative strike-slip displacements recorded along the San Andreas (≧150 km; e.g., Hill, 1981; Powell, 1981; Frizzel *et al.*, 1986) and the San Jacinto (25 km; Sharp, 1967) faults also differ markedly (Fig. 3). The purpose of this brief note is to discuss the possibility that the character of seismicity along major strike-slip faults in southern California is in part a function of cumulative geological offset.

The CIT-USGS southern California seismic network has operated continuously since 1932. The resulting catalog of earthquakes is reportedly complete for earthquakes of $M \geqq 3$ over the entire southern California region, with the exception of the 1933 Long Beach earthquake sequence on the Newport–Inglewood fault (Given *et al.*, 1987). The epicentral distribution of the catalog for the period between January 1932 and February 1986 is plotted in Figure 1. I have drawn boxes around each of the major strike-slip zones in Figure 2. Analysis of seismicity within each of the boxes provides a means to examine the relationship between the character of seismicity and cumulative geological offset along the major strike-slip faults of southern California.

The cumulative number of earthquakes greater than or equal to a given magnitude is plotted versus magnitude for the Newport–Inglewood, Elsinore, San Jacinto, Garlock, and San Andreas fault zones in Figure 4a. Above the magnitude detection threshold ($M3$ in this case), magnitude–frequency curves as shown in Figure 4a are generally characterized by the Gutenberg–Richter relation $\log N = a - bM$, where $N$ is the number of earthquakes with magnitude greater than or equal to the magnitude $M$ and $a$ and $b$ are empirical constants (Ishimoto and Iida, 1939; Gutenberg and Richter, 1944). The value $b$ is the slope of the curve and reflects the relative number of larger to smaller earthquakes. The $b$ value and associated confidence limits to 1 standard deviation are computed for each fault zone using the maximum-likelihood method of Aki (1965) and listed in Table 1. The parameter $a$ is the productivity and empirically defined here as the total number of earthquakes recorded above magnitude 3 during the period of recording. The $b$ value is sensitive to the occurrence of the largest earthquakes along a fault zone. Because the time period sampled by the CIT-USGS catalog is generally less than the expected return time of the largest earthquakes on the faults, a comparison of $b$-values between the faults is of questionable significance. The measure of productivity is a more robust basis for comparison since it is dominated by the relatively greater occurrence rate

of smaller earthquakes. For that reason, I will herein limit my attention to the measures of productivity.

The productivity $a$ of a fault zone will be a function of both the fault length and the rate of strain accumulation. Toward isolating the possible effect of cumulative geological offset on seismic productivity, it is necessary to account for differences in fault length and strain accumulation rate that exist between the faults. Geological estimates of fault slip rate during late Holocene time provide a measure of the rate of strain accumulation and values of fault length may readily

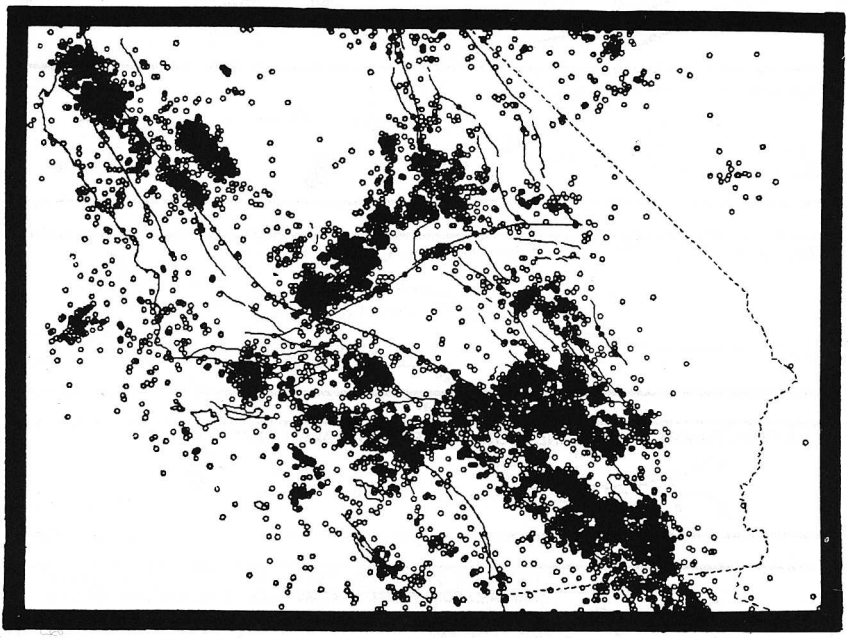

FIG. 1. Epicentral map of southern California seismicity ($M \geqq 3$) recorded by the CIT-USGS seismic network during the period from January 1932 through February 1986.

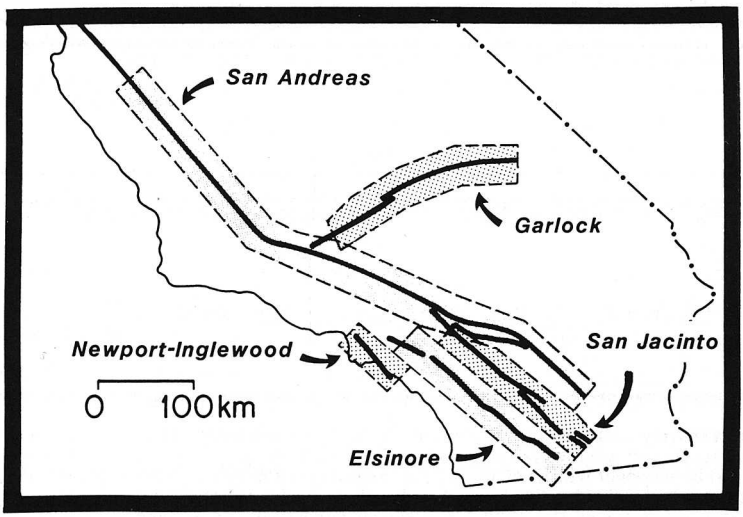


FIG. 2. The polygons encompass the major strike-slip fault zones of southern California.

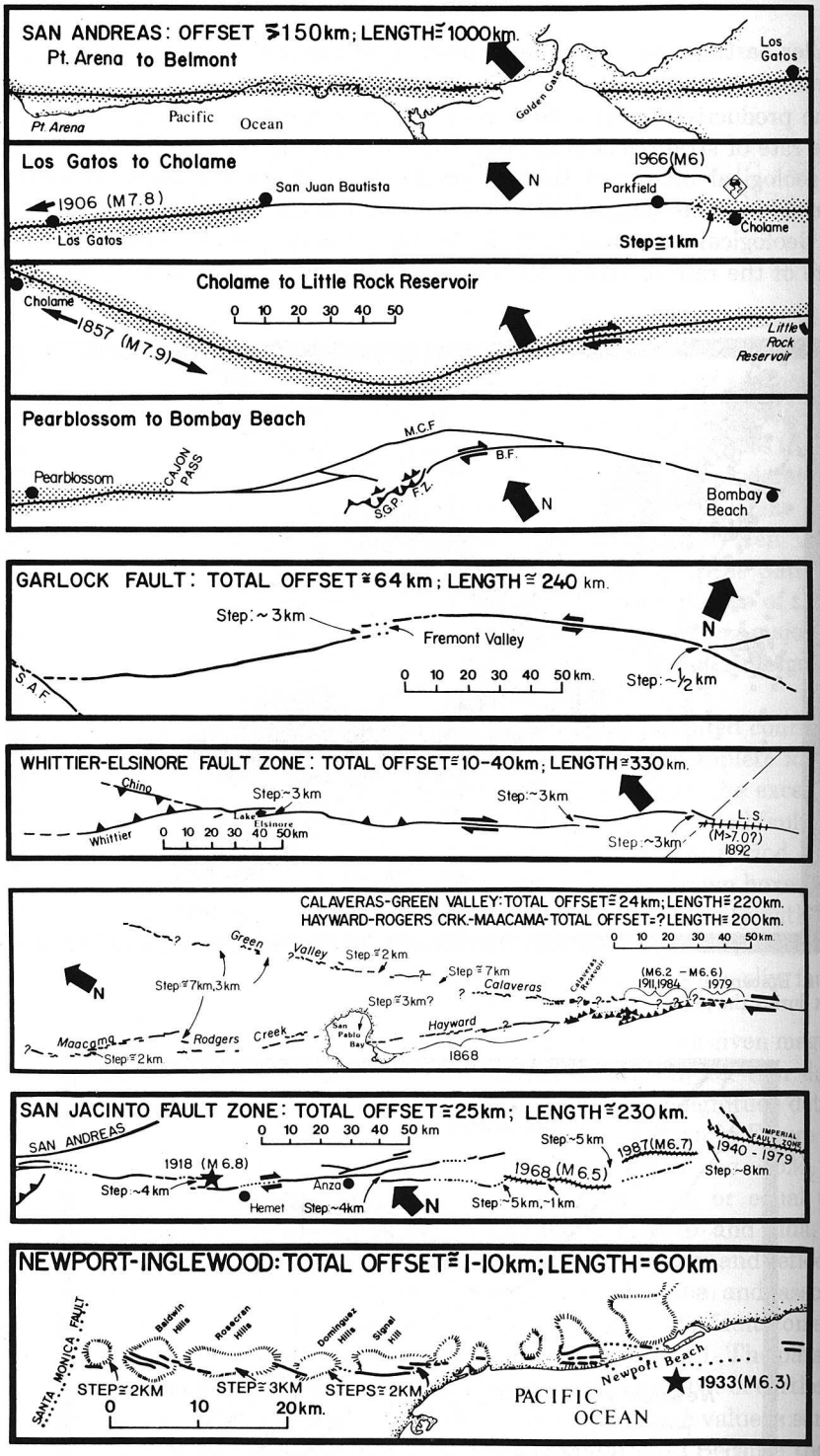


FIG. 3. Maps of major strike-slip faults shown in Figure 2, arranged from bottom to top according to the increasing cumulative geological offset, show the locations and sizes of steps in fault traces which are characterized by stepover widths of $W_s \geqq 1$ km. Segments of fault that have ruptured during historical earthquakes are marked by hachures, stippling or brackets, and the dates and magnitudes of the respective earthquakes. The epicenter of the 1933 Long Beach earthquake is marked by a star, and half-sided arrows indicate sense of displacement along faults. Source of references for this figure are Wesnousky (1988, 1989).

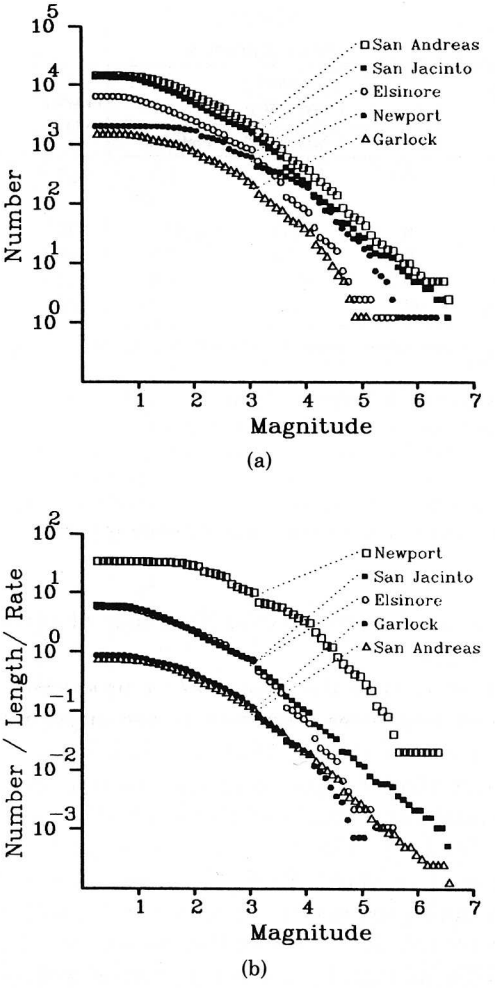


FIG. 4. (a) Number of earthquakes greater than or equal to given magnitude during the period January 1932 through February 1986 for major strike-slip fault zones in southern California. Curves are computed using seismicity within respective boxes shown in Figure 1. The magnitude frequency curves are further normalized in (b) to fault length and fault slip rate (Table 1).

be obtained from fault maps (Fig. 3, Table 1). Thus, the magnitude–frequency curves plotted in Figure 4b are normalized to fault length and fault slip rate. The normalized values of productivity are further plotted versus cumulative geological offset in Figure 5a. The uncertainty bars in Figure 5a are a direct function of the limits on slip rate placed on each fault by geological studies. The relatively large uncertainty bars observed for some of the faults reflect the large variation between the maximum and minimum estimates of slip rate assessed by individual investigators (Table 1; Wesnousky, 1986). There is generally a value of slip rate that is most preferred or accepted by the geological community (e.g., Clark *et al.*, 1984), and it is that rate which is used to compute the preferred value of productivity that is represented by the solid dots in Figure 5a. The productivity, when plotted in the manner of Figure 5a, is a decreasing function of geological offset. The parallel nature of the curves in Figure 4b shows that the observed decrease in productivity

TABLE 1

PLEASE SUPPLY

| Fault | Offset* (km) | Slip Rate† (mm/yr) | | | Length‡ (km) | $b$ (SD = 1) | $a$§ |
|---|---|---|---|---|---|---|---|
| | | Minimum | Maximum | Preferred | | | |
| Newport/ Inglewood | 1–10 | 0.1 | 6.0 | 1.0 | 60 | 0.97 ± 0.08 | 498 |
| San Jacinto | 25 | 8. | 12.0 | ≧10. | 230 | 0.92 ± 0.03 | 1330 |
| Elsinore | 10–40 | 0.6 | 9.0 | 4.0 | 280 | 1.22 ± 0.05 | 661 |
| Garlock | 240 | 0.7 | 30. | 7.0 | 240 | 0.97 ± 0.08 | 164 |
| San Andreas | ≧150¶ | 25. | 33. | 33.0 | 600 | 0.85 ± 0.02 | 1702 |

* Values of cumulative geologic offset taken from summary by Wesnousky (1988) and Morton and Miller (1987).

† Values of fault slip rate taken from summary by Wesnousky (1986).

‡ Values correspond to fault lengths within boxes in Figure 1.

§ Sum of $M \geqq 3$ events recorded between January 1932 and February 1986.

¶ Powell (1981) and Frizzel *et al.* (1986) place cumulative offset across the currently active trace of the San Andreas fault at about 150 km. Cumulative offset across the entire San Andreas system including both currently active and inactive traces is estimated at ≧250 km (e.g., Hill, 1981).

with offset shown in Figure 5 is stable over the range of threshold magnitudes up to between magnitude 4 and 5.

Some question may exist that the measures of productivity are biased by the occurrence of aftershock sequences attendant to the larger main shocks along the fault traces. During the period 1932 to 1986, the San Jacinto fault produced three $M \geqq 6$ earthquakes: the $M6.5$ Borego Mountain earthquake of 9 April 1968; the $M6.2$ Santa Rosa Mountain earthquake of 19 March 1954; and an $M6.5$ earthquake on 21 October 1942. Similarly, the Newport-Inglewood fault produced the $M6.3$ Long Beach earthquake of 11 March 1933. No large earthquakes have occurred on the Whittier–Elsinore fault zone and the southern San Andreas has been absent of large earthquakes but for the $M6.5$ Desert Hot Springs earthquake of 4 December 1948. The open symbols in Figure 5a are the normalized values of productivity computed after removal of 1 year of data subsequent to each of the above listed large shocks, a period sufficient to include the occurrence of most aftershocks. The observed decrease in productivity as a function of fault offset also remains after removal of the aftershock sequences.

To summarize, seismic productivity on the faults is observed to be a systematic function of geological offset. Withstanding observations that spatial variations in heat flow, rock type, and hydrology will also affect the character of seismicity along strike of fault zones, the data in Figure 5a suggest that cumulative offset may play a fundamental role in controlling the average seismic productivity of strike-slip fault zones. In some sense, the seismic productivity, being dominated by the occurrence of smaller earthquakes, which reflect only a minor fraction of seismic energy release along a fault zone, may only be viewed as a description of seismic noise along the fault zones. In that regard, a physical interpretation to the observed decrease in productivity as a function of fault slip may lie in the observation that the trace of a strike-slip fault is generally complex, characterized by a zone of discrete fault segments, each of which is separated from the next segment by a step in the fault trace (Fig. 3).

Steps in fault trace can be characterized by the width $W_s$ of the step as measured perpendicular to the fault zone. A simple but quantitative measure of fault trace

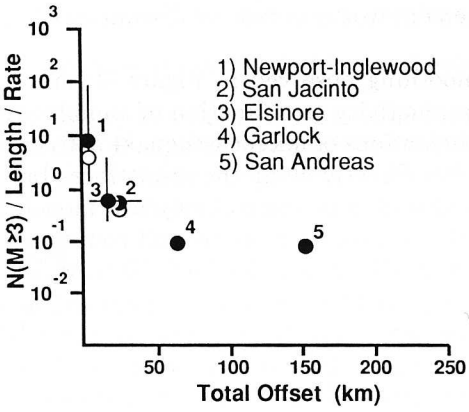


(a)

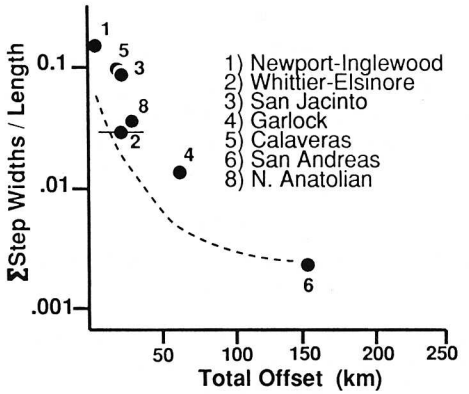


(b)

FIG. 5. (a) The seismic productivity (sum of events with $M \geqq 3$ during the period from 1932 to 1986) normalized to fault length and fault slip rate is plotted (solid symbols) as a function of cumulative fault offset for major strike-slip faults in southern California. Uncertainty bars directly reflect maximum and minimum estimates of slip rates and solid symbols correspond to preferred estimates of slip rates (see text for further discussion). Open symbols are computed after removal of 1 year of data subsequent to largest ($M \geqq 6$) earthquakes during the period from 1932 to 1986. Lack of open symbol indicates that no $M \geqq 6$ events were recorded between 1932 and 1986. (b) Fault trace complexity measured as the cumulative sum of step widths ($\sum W_s$; closed symbols) per unit length of fault trace is plotted versus cumulative geologic offset for major strike-slip faults in California and northern Turkey (see Table 1). The dashed line marks the trend observed if only the number of steps per unit fault length is used as the measure of fault trace complexity.

complexity is the number of steps of given $W_s$ or greater per unit fault length ($l$). Similarly, one may plot the sum of fault step widths per unit fault length ($\sum W_s/l$) as a measure of fault trace complexity. In a separate study, I recently compiled maps showing both the locations and sizes of all steps of $W_s \geqq 1$ km along the length of major strike-slip faults in California and Turkey (Wesnousky, 1988). The fault maps in Figure 3 are taken from that study. I also plotted the number of steps per unit fault length vesus cumulative geological offset for the respective faults. I repeat that result in Figure 5b in addition to a plot of the sum of step widths $\sum W_s$ versus fault length. The complexity of fault trace when plotted in this manner is a decreasing function of geological offset, consistent with the idea that fault zones are characterized by a discontinuous trace during early stages of development and

that increasing displacement works to remove discontinuities, effectively smoothing the fault trace.

The structural smoothing observed in Figure 5b may be responsible for the observed decrease in productivity as a function of cumulative fault offset (Fig. 5a). More specifically, concentrations of microearthquake activity along strike-slip faults are commonly located not directly along the fault traces but within the vicinity of steps or other complexities in fault trace. Analytical models further show that the far-field stresses that drive tectonic motions will concentrate near steps or other complexities in fault traces (Segall and Pollard, 1980) which, when taken with the previous observation, suggests that the level of seismicity along strike-slip faults is controlled in part by the heterogeneity of the stress-field within the vicinity of the faults. Hence, it seems a reasonable hypothesis that the observed decrease in seismic productivity with cumulative geologic offset may reflect a structural smoothing of the faults and, hence, a smoothing of the stress field within the vicinity of strike-slip faults as offset grows.

## Acknowledgments

Special thanks goes to Paul Reasenberg for checking as well as correcting some of my calculations and to Lucy Jones for providing me access to the CIT-USGS data set. I also thank Craig Nicholson for his thorough review of this note, John Anderson for his useful comments, and Ingrid Ramos for typing the manuscript. The research was supported by NSF Grant EAR-8816136.

## References

Aki, K. (1965). Maximum likelihood estimate of $b$ in the formula $\log N = a - bM$ and its confidence limits, *Bull. Earthquake Res. Inst., Univ. Tokyo* **43,** 237–239.

Allen, C. R. (1968). The tectonic environments of seismically active and inactive areas along the San Andreas fault system, in *Proc. Conference on Geologic Problems of San Andreas Fault System*, W. R. Dickenson and A. Grantz (Editors), Stanford University Press, Stanford, California, 70–82.

Clark, M. M., K. K. Harms, J. J. Lienkaemper, D. S. Harwood, K. R. Lajoie, J. C. Matti, J. A. Perkins, M. J. Rymer, A. M. Srna-Wojcicki, R. V. Sharp, J. D. Sims, J. C. Tinsley, and J. I. Ziony (1984). Preliminary slip-rate table for late Quaternary faults of California, *U.S. Geol. Surv. Open-File Rep. 84-106*, 12.

Frizzel, V. A., Jr., J. M. Mattison, and J. C. Matti (1986). Distinctive Triassic megaporphyritic monzogranite: evidence for only 160 kilometers of offset along the San Andreas Fault, southern California: *J. Geophys. Res.* **91,** 14,080–14,088.

Given, D., L. Hutton, and L. M. Jones (1987). The southern California Network Bulletin July–December, 1986, *U.S. Geol. Surv. Open-File Report 87-488*, 28.

Gutenberg, B. and C. F. Richter (1944). Frequency of earthquakes in California, *Bull. Seism. Soc. Am.* **34,** 185–188.

Hill, M. L. (1981). San Andreas fault: history of concepts, *Geol. Soc. Am. Bull.* **92,** 112–131.

Ishimoto, M. and K. Iida (1939). Observations sur les seism enregistre par le microseismograph construite dernierment (I) (with Japanese summary), *Bull. Earthquake Res. Inst., Univ. Tokyo* **17,** 443–478.

Kanamori, H. and C. R. Allen (1986). Earthquake repeat time and average stress drop, in *Earthquake Source Mechanics*, vol. 37, S. Das, J. Boatwright, C. H. Scholz (Editors), Washington, D.C. 157–167.

Morton, D. and F. Miller (1987). K/AR apparent ages of plutonic rocks from the northern part of the peninsular ranges batholith, southern California, *Geol. Soc. Am. Abstr. Prog., Cordilleran Section* **19,** 435.

Powell, R. E. (1981). Geology of the crystalline basement complex, eastern transverse ranges, southern California: constraints on regional tectonic interpretations, *Ph.D. Thesis*, California Institute of Technology, Pasadena, California, 441 pp.

Sanders, C. O. and H. Kanamori (1984). A seismotectonic analysis of the Anza seismic gap, San Jacinto fault zone, southern California, *J. Geophy. Res.* **89,** 5873–5890.

Segall, P. and D. D. Pollard (1980). Mechanics of discontinuous faults, *J. Geophys. Res.* **85,** 4337–4350.

Sharp, R. V. (1967). San Jacinto fault zone in the peninsular ranges of southern California, *Geol. Soc. Am. Bull.* **78,** 705–730.

Wesnousky, S. G. (1986). Earthquakes, quaternary faults, and seismic hazard in California, *J. Geophys. Res.* **91,** 12587–12631.

Wesnousky, S. G. (1988). Seismological and structural evolution of strike-slip faults, *Nature* **335,** 340–343.

Wesnousky, S. G. (1989). Seismicity and the structural evolution of strike-slip fault zones, in *Proc. Conf. XLV on Fault Segmentation and Controls of Rupture Initiation and Termination*, D. P. Schwartz and R. H. Sibson (Editors), *U.S. Geol. Surv. Open-File Rep. 89-315*, 193–228.

CENTER FOR NEOTECTONIC STUDIES
MACKAY SCHOOL OF MINES
UNIVERSITY OF NEVADA, RENO
RENO, NEVADA 89557-0135

Manuscript received 2 January 1990